

Published in final edited form as:

J Neuroimmunol. 2010 September 14; 226(1-2): 81–92. doi:10.1016/j.jneuroim.2010.05.034.

Distinct macrophage subpopulations regulate viral encephalitis but not viral clearance in the CNS

Christina D. Steel^{*}, Woong-Ki Kim^{*}, Larry Sanford[†], Laurie Wellman[†], Sandra Burnett[‡], Nico Van Rooijen[§], and Richard P. Ciavarra^{*,1}

Christina D. Steel: steelcd@evms.edu; Woong-Ki Kim: kimw@evms.edu; Larry Sanford: sanfordl@evms.edu; Laurie Wellman: wellmall@evms.edu; Sandra Burnett: Sandra.h.burnett@gmail.com; Nico Van Rooijen: nvanrooijen@clodronateliposomes.org

^{*} Department of Microbiology and Molecular Cell Biology, Eastern Virginia Medical School, Norfolk, Virginia, USA [†] Department of Pathology and Anatomy, Eastern Virginia Medical School, Norfolk, Virginia, USA [‡] Department of Microbiology and Molecular Biology, Brigham Young University, Provo, Utah, USA [§] Department of Molecular Cell Biology, Faculty of Medicine, Vrije Universiteit, Amsterdam, The Netherlands

Abstract

Intranasal application of vesicular stomatitis virus (VSV) induces acute encephalitis characterized by a pronounced myeloid and T cell infiltrate. The role of distinct phagocytic populations on VSV encephalitis was therefore examined in this study. Ablation of peripheral macrophages did not impair VSV encephalitis or viral clearance from the brain, whereas, depletion of splenic marginal dendritic cells impaired this response and enhanced morbidity/mortality. Selective depletion of brain perivascular macrophages also suppressed this response without altering viral clearance. Thus, two anatomically distinct phagocytic populations regulate VSV encephalitis in a non-redundant fashion although neither population is essential for viral clearance in the CNS.

Keywords

microglia

1. Introduction

Vesicular stomatitis virus (VSV) is a neurotrophic ssRNA virus of the Vesiculovirus genus in the Rhabdoviridae family and is the prototypic virus of this family that includes rabies virus. Following systemic infection, immunocompetent mice rapidly clear VSV from peripheral organs, produce IgM and neutralizing IgG antibodies and mount a robust CTL response although viral antigens persist for weeks in peripheral tissues. (Battegay et al., 1996; Charan et al., 1986; Turner et al., 2007). When VSV is delivered via the intranasal route, it initially infects and replicates in olfactory receptor neurons and is then transmitted via the olfactory nerve to the central nervous system (CNS) within 12–24 hours (Forger et al., 1991; Reiss et al., 1998). VSV replicates invasively in the olfactory bulb (OB)

¹Corresponding author: Dr. Richard P. Ciavarra, Department of Microbiology and Molecular and Cell Biology, Eastern Virginia Medical School, 700 W Olney Road, Norfolk, VA 23501. Phone 757-446-5661; fax 757-624-2255; ciavarrp@evms.edu.

Publisher's Disclaimer: This is a PDF file of an unedited manuscript that has been accepted for publication. As a service to our customers we are providing this early version of the manuscript. The manuscript will undergo copyediting, typesetting, and review of the resulting proof before it is published in its final citable form. Please note that during the production process errors may be discovered which could affect the content, and all legal disclaimers that apply to the journal pertain.

penetrating deeper layers of this structure, reaching the OB ventricle by days 4–5 post infection producing focal cytopathology. Depending on the dose and strain, virus can enter the ventricles causing inflammation and necrosis around the ventricles and travel caudally to the hindbrain by day 8 post infection VSV does not use the trigeminal nerve for entry into the brain, as the trigeminal ganglion remains virus-free following intranasal infection. Although VSV infection of the CNS is associated with a high rate of morbidity and mortality, surviving mice completely clear infectious virus from the brain around days 10–12.

The observation that some mice survive CNS infection with this virus suggests that innate and adaptive antiviral mechanisms are activated in the CNS. With respect to innate immunity, prior immunohistochemical studies by Reiss and colleagues indicated that intranasal infection with VSV activated glial cells (astrocytes, microglia) initially in the OB and induced expansion of these resident cell populations (Bi et al., 1995). Activation of astrocytes and microglia was likely responsible for the reported T cell-independent encephalitis seen with this virus (Frei et al., 1989; Nansen et al., 2000). In addition to the innate response in the CNS, adaptive immunity also contributes to host resistance because SCID and nude mice invariably succumb to a fatal encephalitis but can be rescued by adoptively transferred T cells (Coons et al., 1991; Hummer et al., 1990). Similarly, antibody-mediated depletion of CD8⁺ or CD4⁺ T cells renders mice susceptible to VSV replication and dissemination to the CNS (Huneycutt et al., 1993). According to the current paradigm, T cells activated in the draining cervical lymph node (CLN) navigate through the blood brain barrier (BBB) to mediate their antiviral effector functions. Although the precise mechanism(s) by which T cells extravasate through the vascular endothelium and enter the CNS parenchyma are not fully understood, several adhesion molecules such as CD11a (LFA-1), CD11b (Mac-1) and CD49d (VLA-4) are upregulated on T cells isolated from brains of VSV infected mice (Steel et al., 2009). Once VSV-activated T cells penetrate the BBB, they are thought to follow CC and CXC chemokine gradients produced in the encephalitic brain (Ireland and Reiss, 2006) to localize at sites of virus replication and/or antigen deposition, a view consistent with immunohistochemical studies. It should be noted that VSV globally activates T cells irrespective of antigen specificity. For example, 24 hours post infection, the majority of CD8⁺ and to a lesser extent CD4⁺ T cells express CD69 and CD25 (unpublished observation) and this far exceeds estimated precursor frequencies for VSV-specific T cells (Ciavarrà and Tedeschi, 1994). Even at the peak of the CD8⁺ T cell response in the brain, $\leq 30\%$ of CD8⁺ T cells are specific for the single immunodominant nuclear protein epitope (VSV-N_{52–59}) although the vast majority of CD8⁺ T cells express late activation antigens CD49d (VLA-4) and CD11a (Steel et al., 2009). Thus, the specificity of a significant fraction of CD8⁺ T cells that infiltrates the CNS following infection with VSV remains to be clarified.

We have previously reported a multi-colour flow cytometric characterization of the cells that infiltrate the brain during VSV encephalitis in normal mice and mice rendered deficient of peripheral DCs (Steel et al., 2009). In this report we extend these studies to examine how distinct populations of macrophages (m Φ) regulate VSV encephalitis and viral clearance in the brain.

2. Materials and Methods

Mice and virus infection

Breeding pairs of macrophage fas-induced apoptosis (MAFIA) mice were purchased from Jackson Laboratories (Bar Harbor, ME) and subsequently bred in-house. These mice express a bicistronic mRNA encoding both EGFP and transgenic cytoplasmic Fas domains under the control of the *c-fms* promoter (Burnett et al., 2004). Mice were phenotyped for endogenous

EGFP by flow cytometry performed on blood obtained by tail prick. Mice lacking EGFP expression were used as controls. Wild-type VSV-Indiana strain, provided by Dr. Philip Marcus, University of Connecticut, was grown and assayed as previously described (Marvaldi et al., 1977). Virus was grown in confluent monolayers of Vero cells and virus titers determined by standard plaque assays (Sekellick and Marcus, 1979). VSV was introduced into the brain via intranasal application of 5 μ l/nostril with either 5 \times 10⁴ (male) or 2 \times 10⁵ (female) PFU VSV (Barna et al., 1996). All experiments were performed in accordance with federal guidelines and under an Institutional Animal Care and Use Committee-approved protocol.

Cell isolation and depletion

Brains were excised, individually homogenized and then subjected to discontinuous Percoll centrifugation to enrich for microglia and leukocytes as previously described (Steel et al., 2009). Single cell suspensions of peripheral organs (spleen, draining cervical lymph nodes (CLNs), lung) were scrubbed through 40 μ nylon mesh cell strainers. Erythrocytes were lysed as necessary using BD PharmLyse Ammonium Chloride lysing reagent (Becton Dickinson, Carlsbad, CA). Peripheral m Φ depletion was achieved by administration of five consecutive intravenous injections of 10mg/kg AP20187 (Ariad Pharmaceuticals, Cambridge, MA) via the lateral tail vein or the retro-orbital venous sinus as previously described [5]. Alternatively, mice were depleted of peripheral m Φ by a single intravenous (retro-orbital sinus) injection of liposome-encapsulated Cl2MBP (dichloromethylene bisphosphonate, clodronate) kindly provided by Roche Diagnostics GmbH, Mannheim, Germany. Depletion of brain PVMs (PVM) was achieved by intracerebroventricular (ICV) injection of clodronate following a previously reported protocol (Galea et al., 2005). Briefly, following induction mice were weighed and the surgical site prepared by shaving, swabbing with betadine and a final swab with 70% ethanol. Mice given subcutaneous injections of potassium penicillin (100 IU/g body weight, 100 μ L) and gentamicin (0.005 mg/g body weight, 100 μ L) prior to surgery were then placed in a stereotaxic frame. An incision was made along the coronal suture and the scalp was retracted. The position of the left lateral ventricle was determined relative to the bregma as AP -0.5 mm, ML -1.0 mm, and DV -2.0mm. A small hole was drilled into the skull and clodronate infused at a rate of 0.67 μ L/min for 12 min (8 μ L per mouse). The skull was filled with bone wax and the scalp sutured. Mice were allowed to recover for 3 days prior to experimental manipulation. Table 1 indicates the cell populations reported to be depleted following the indicated treatment.

Multicolour Flow Cytometry

Unless indicated otherwise, monoclonal antibodies (mAbs) against cell surface antigens were purchased from eBioscience (San Diego, CA). Cells were stained and washed in flow cytometry wash buffer (PBS supplemented with 1% goat serum and 0.1% sodium azide). The following mAbs were used in this study: CD11b, clone M1/70; CD45, clone 30-F11; MHC II, clone M5/114.15.2; CD11c, clone N418; CD4, clone GK1.5; CD8 α , clone 53-6.7; CD49b, clone DX5; CD45R, clone RA3-6B2; MHC I, clone 34-1-2S; PD-1, clone J43; CD49d, clone R1-2; CD115, clone AFS98; CD40, clone 1C10; CCR7, clone 4B12; and CD80, clone 16-10A1. PDCA-1 (clone JF05-1C2.4.1) was purchased from Miltenyi Biotec, Auburn, CA. Tetramers directed against the immunodominant VSV nucleocapsid protein (VSV-N₅₂₋₅₉, RGYVYQGL) were obtained from the NIH Tetramer Core Facility. Fluorophore conjugates varied based on staining profiles used. Acquisition of 20–200,000 events was performed using a Becton Dickinson (San Diego, CA) FACSCalibur using CellQuest software (v3.3, Becton Dickinson). Acquired cells were analyzed using FlowJo software (Tree Star, Ashland, OR). Non-specific binding in the absence of additional Fc block was previously evaluated and did not affect staining patterns. To determine the absolute number of microglia and infiltrating leukocytes in the CNS, a leukocyte gate was

first defined for these cells based on forward and side scatter characteristics. Preliminary studies verified that these gated cells were CD45⁺ and viable ($\geq 95\%$ propidium iodide and annexin negative). The percentage of microglia (CD45^{low/int}) or infiltrating blood cells (CD45^{high}) within this gate was then used to calculate cell recoveries. All gates and quadrants were established with the use of appropriate isotype controls.

3. Results

To access the efficacy of m Φ depletion, MAFIA mice were treated with dimerizer and at the indicated times peritoneal exudates cells (PECs) were evaluated by microscopy and flow cytometry. It is apparent from Figure 1 that EGFP⁺ PECs isolated from untreated mice were primarily m Φ because of high EGFP expression (panel b), histological appearance (panel c) and F4/80 expression (data not shown). EGFP^{low} cells were also primarily m Φ as judged by histological criteria (data not shown). As expected, AP20187 treatment markedly depleted EGFP^{high} cells (panel e). The remaining EGFP⁺ cells displayed high autofluorescence and were primarily foamy and apoptotic m Φ (panel f). Dimerizer treatment was associated with increased numbers of peritoneal EGFP^{low} cells (panel e). When sorted, these cells had the morphology of granulocytes or band cells (panel g) and expressed the monocyte/granulocyte marker Gr-1 (panel h). EGFP^{low}Gr-1⁺ cells remained the predominant population in the peritoneum for at least two-week post depletion (panel i). Thus, AP20187 treatment depletes primarily EGFP^{high} m Φ . The peritoneum is then repopulated primarily by EGFP^{low} cells with a morphology and phenotype characteristic of granulocytes.

VSV encephalitis in MAFIA mice and MAFIA mice rendered deficient of peripheral macrophages

We previously reported that VSV encephalitis is characterized by a prominent CD45^{high}CD11b⁺ infiltrate in the brain, a phenotype typically associated with m Φ (Ciavarra et al., 2006). We therefore sought to determine the functional importance of peripheral m Φ in the antiviral immune response in the CNS and whether this infiltrate was derived from circulating monocytes. To address these questions, MAFIA mice were treated with AP20187 to deplete cells of the monocytes/m Φ lineage (Burnett et al., 2004) and the following day given a single intranasal application of VSV. Control MAFIA mice were given just VSV or AP20187. Treatment of MAFIA mice with AP20187 alone did not diminish resident CD45^{low/int}CD11b⁺ microglia relative to untreated B6 mice (Figure 2, box panels a–d). Two populations of MAFIA microglia were detected based on EGFP expression (see Figure 3, panels a–c), an observation consistent with high ($\geq 50\%$) expression of CD115 (colony stimulating factor receptor-1) on microglia from mock and VSV infected mice (unpublished observation). VSV induced upregulation of microglial MHC class II antigens and this activation occurred independent of peripheral m Φ (panels e–h). Microglia remained uniformly F4/80⁺Gr-1⁻ even at the peak of the inflammatory response (unpublished observation). Despite depletion of peripheral monocytes/macrophages, a pronounced population of CD45^{high}CD11b⁺ cells still accumulated in the brains of these mice (compare panels a–d). Further characterization revealed a trace population of resident DCs (CD11c⁺) in naive mice that expanded modestly in both virus-infected groups. Whether brain associated DCs are derived from blood DCs or immature monocytes that differentiate into DCs once in the brain parenchyma remains to be determined. Plasmacytoid DCs (CD11c⁺PCDA-1⁺) were not detected in encephalitic brains at any time following infection with VSV (panels i–l). Ablation of peripheral m Φ did not impair the accumulation of CD8⁺ T cells in the CNS. Tetramer staining revealed two CD8⁺CD49d⁺ expanded populations induced by VSV irrespective of dimerizer treatment, one specific for VSV (tetramer⁺) and a second with unknown specificity (Figure 2, tetramer⁻, panels m–p). Mice depleted of m Φ remained healthy during the course of this experiment indicating efficient viral clearance

from the CNS, whereas two VSV infected mice developed hind limb paralysis 6 days post infection. We observed no significant differences in survival rates between intact and dimerizer treated MAFIA following intranasal application of VSV. Thus, these data demonstrate that acute depletion of peripheral m Φ does not impair VSV encephalitis or clonal expansion of CD8⁺ T cells including the subset specific for immunodominant epitope of VSV. Similar conclusions are reached when data are calculated as absolute cell recoveries (Figure 2, panel B).

Macrophage depletion is associated with a pronounced and sustained granulocytic response in haematopoietic and non-haematopoietic tissues during VSV encephalitis

The presence of a pronounced infiltrate of CD45^{high}CD11b⁺ cells in the brains of VSV infected MAFIA given dimerizer raised the possibility that m Φ depletion was either not efficient or sustained in virus-infected animals. Alternatively, the CD45^{high}CD11b⁺ infiltrate may not contain m Φ but another cell type like granulocytes that also express this phenotype. To examine the former possibility, we repeated the experiment and also evaluated the extent to which CD45^{high}CD11b⁺ cells remained depleted in the peritoneum and bone marrow during the peak of the encephalitic response. As demonstrated previously, depletion of peripheral m Φ did not alter the encephalitic response (Figure 3, panels a–c and data not shown). Analysis of the peritoneum of these mice indicated that naïve mice contained a prominent population of CD45^{high}CD11b⁺ cells that diminished modestly and then expanded in mice given VSV or VSV plus dimerizer, respectively (panels d–f and Figure 3B). This population contained both EGFP^{low/int} and EGFP^{high} subsets, the latter markedly diminished by VSV infection and was no longer detectable in mice given dimerizer and VSV (panels g–i). The EGFP^{low/int} population was more stable in VSV infected mice and expanded slightly in mice given both dimerizer and VSV. CD45^{high}CD11b⁺EGFP^{low/int} cells were predominately Gr-1⁻ indicating that these cells were likely immature m Φ and not granulocytes (panels g–i). Thus, the peritoneum of VSV infected mice given dimerizer remained essentially devoid of m Φ (CD45^{high}CD11b⁺Gr-1⁻EGFP^{high}) even 8 days post dimerizer treatment. There appeared to be a compensatory increase in immature m Φ (CD45^{high}CD11b⁺Gr-1⁻EGFP^{low/int}) in the peritoneum. Similar conclusions were reached when total cell recoveries were calculated (Figure 3, panel B). In the haematopoietic bone marrow, the number of CD45^{high}CD11b⁺ cells remained fairly stable regardless of the experimental manipulation (panels j–l and Figure 2C). In naïve MAFIA mice, this CD45^{high}CD11b⁺ population contained only a EGFP^{low/int} subset that was markedly reduced in virus-infected animals but expanded in the dimerizer treated group (panel m–o). In contrast to the peritoneum, virtually all CD11b⁺ cells in the bone marrow expressed Gr-1. When cells recoveries were calculated for these different populations, similar conclusions were reached (Figure 3C). Thus, dimerizer treatment results in the sustained elimination of peripheral m Φ (CD45^{high}CD11b⁺EGFP^{high}Gr-1⁻) even in virus-infected mice. The bone marrow mounts a potent compensatory response composed primarily of granulocytes (CD45^{high}CD11b⁺Gr-1⁺EGFP^{low/int}) some of which may migrate into the encephalitic brain.

VSV encephalitis is impaired in mice given liposome-encapsulated clodronate

To further characterize the CD45^{high}CD11b⁺ infiltrate and to compare studies in the MAFIA model with an established procedure for depletion of blood monocytes and tissue m Φ , MAFIA mice were given a single intravenous injection of liposome-encapsulated clodronate. This “suicide” technique depletes cells of the monocyte/m Φ lineage in the bone marrow, spleen and liver but not peripheral lymph nodes including the draining cervical lymph nodes (CLNs) (Van Rooijen et al., 1990). The following day mice were given an intranasal instillation of VSV and 7 days post infection the cellular infiltrate was analyzed by 4-color flow cytometry. Microglia isolated from naïve mice remained uniformly F4/80⁺,

did not express the granulocytic marker Gr-1 and sustained this CD45^{low/int}CD11b⁺F4/80⁺Gr-1⁻ phenotype in the encephalitic brain (data not shown). VSV induced a pronounced infiltrate dominated by CD45^{high}Gr-1⁺F4/80⁻EGFP^{+/-} cells, a phenotype characteristic of neutrophils and not mΦ (Figure 4, panels a-l). Clodronate treatment markedly suppressed this response as well as the infiltration of conventional myeloid (CD8⁻) and lymphoid (CD8⁺) DCs (panels m-r). Encephalitic brains contained a CD11c⁻PDCA-1⁺ population whose lineage and function will require further investigation. Clodronate treatment also inhibited the accumulation of CD8⁺ T cells (panels p-r) including VSV-specific T cells (panels s-u) in the CNS. Similar conclusions were reached when cell recoveries were calculated from multiple experiments (panels B, C). Thus, in striking contrast to the MAFIA model, liposome-encapsulated clodronate profoundly suppressed VSV encephalitis. In addition, clodronate-treated mice showed increased morbidity and mortality relative to mice given just VSV. Half of the mice (3/6) died at 6 days post-infection (two days earlier than typical onset of morbidity for this strain) and by 7 days post-infection the remaining mice were moribund, while untreated VSV-infected mice showed only early signs of pathogenesis (panel D). Morbidity/mortality was not correlated with impaired viral clearance (panel E). Intravenous administration of clodronate does not deplete phagocytic cells in peripheral lymph nodes and lungs and would not be expected to alter T cell activation and clonal expansion in these locations. Consistent with these observations, normal numbers of CD8⁺VSV-N T cells were detected in the CLN (panel F) and lungs (data not shown). As expected, clodronate inhibited expansion of VSV-N T cells in the spleen (data not shown).

Production of IFN-γ in the CNS is dependent on peripheral macrophages

To further examine the potential functional role of mΦ in the encephalitic brain, the primary VSV-induced IFN-γ response was assessed in normal mice and mice rendered deficient of mΦ by intravenous administration of liposome-encapsulated clodronate. Figure 5 demonstrates that only trace numbers of IFN-γ-secreting cells were detected in the brain of naïve MAFIA mice. However, this population expanded in the brains of VSV infected mice, whereas clodronate treatment prior to virus infection markedly suppressed this response. This was true when data was expressed either as the number of ELISPOTS/10⁵ cells or total number of ELISPOTS per brain (top and bottom panels, respectively). These data contrast with prior studies where ablation of peripheral DCs *in vivo* failed to suppress this response in the CNS (Ciavarrá et al., 2006). The observation that the VSV-induced IFN-γ response is normal in mice with a markedly reduced infiltrate following DC depletion suggests that a resident cell type produces this cytokine. Why peripheral mΦ but not DCs are required for this response remains to be clarified.

Perivascular and meningeal macrophages play an essential role in VSV encephalitis

Macrophages have documented APC activity *in vivo* (Pozzi et al., 2005) and within the CNS, PVM are believed to be the foremost APC, a function ideally suited for their strategic location at the BBB between the endothelial basement membrane and the glia limitans. Clodronate-encapsulated liposomes are selectively engulfed by cerebral PVM/MM leading to progressive intracellular accumulation of sodium clodronate that kills PVM by day 5 as a result of adenosine triphosphate depletion (Russell and Rogers, 1999) and apoptosis (van Rooijen et al., 1996). That PVM/MM can function as APCs is supported by the observation that selective depletion of PVM and MM *in vivo* with clodronate mitigates clinical symptoms associated with experimental allergic encephalomyelitis (EAE) and bacterial meningitis (Polfliet et al., 2002; Polfliet et al., 2001b). To test whether VSV encephalitis is dependent on these cells, we performed an ICV infusion of clodronate-encapsulated liposomes following previously reported procedures. Mice were rested 3 days and then infected with VSV via the intranasal route. VSV encephalitis was characterized 7 days post

infection by flow cytometry (Figure 6A) and quantified based on calculated cell recoveries (panels B, C). It is apparent from this study that ICV clodronate did not deplete resident microglia (R2, panels a, b) or prevent VSV-induced expression of MHC class I antigens on these cells indicating that microglial activation was not dependent on the presence of PVM/MM (panels c, d). However, the inflammatory response was markedly impaired because the accumulation of blood-derived leukocytes (CD45^{high}) was suppressed by clodronate (R3, panels a, b), a response that was primarily granulocytic (panels I, j). Accumulation of CD4⁺ and CD8⁺ T cell subsets as well as CD8⁺ VSV-specific T cells was similarly inhibited by this treatment (panels e–h). Suppression of VSV encephalitis was also apparent when cell recoveries were calculated (panel C). Seven days post-infection, the control mice given just VSV were morbid, with one mouse exhibiting hind-limb paralysis. This mouse still had some residual VSV in the brain although the remaining two moribund mice had undetectable titers (panel D). This suggests that the observed morbidity may be related to the inflammatory response and not to the cytopathic activity of the virus. Mice given ICV clodronate were not moribund with no evidence of hind-limb paralysis and no detectable VSV in their brains. Thus, ICV clodronate markedly suppressed VSV encephalitis and reduced morbidity without altering viral clearance.

4. Discussion

In this report we have utilized two different approaches to assess whether monocytes and tissue mΦ cells play an essential role in VSV encephalitis and viral clearance in the CNS. In the MAFIA model peripheral depletion of mΦ was achieved after 5 daily injections of dimerizer. Depletion was sustained in naïve (uninfected) mice because the peritoneum remained devoid of EGFP^{high} cells for at least two weeks. Although the *c-fms* gene is expressed in mΦ and DCs (Rieser et al., 1998), the suicide gene is expressed an order of magnitude lower in DCs than in mΦ (Burnett et al., 2004; Steel et al., 2008) and this may explain the relative preservation of DCs following dimerizer treatment. Although a subset (~30–40%) of microglia expressed EGFP, these cells remained intact during treatment with dimerizer suggesting that AP20187 does not efficiently cross the BBB. Dimerizer treatment also did not inhibit upregulation of microglial class II antigens and expansion of microglia suggesting that microglia activation was independent of peripheral monocytes/macrophages. Flow cytometric analysis of leukocytes isolated from VSV infected brains revealed a prominent population of CD45^{high}CD11b⁺ cells as well as a smaller infiltrate of CD11c⁺ DCs. At the time points investigated, we did not detect pDCs, B cells or NK cells in encephalitic brains. Despite a relatively small infiltrate of CD45^{high}CD11b⁺-lymphoid cells, CD8⁺ T cells were abundant suggesting activation-induced upregulation of CD11b, a view confirmed by back-gating analysis (data not shown). A significant fraction of CD8⁺ T cells bound tetramers demonstrating specificity for immunodominant nuclear protein epitope. The specificity of the remaining activated T cells remains to be elucidated. Despite their dual functionality as APCs and effector cells, mice rendered deficient of peripheral mΦ mounted a normal inflammatory response in the CNS. Normal accumulation of CD8⁺VSV-N T cells in the brain also implies preservation of peripheral DCs in dimerizer treated mice because depletion of these cells markedly inhibits antiviral immunity and viral clearance (Steel et al., 2009). MAFIA mice remained healthy during the course of this experiment suggesting normal VSV clearance in the CNS in mice rendered deficient of peripheral mΦ.

The presence of a prominent infiltrate of CD45^{high}CD11b⁺ cells raised the possibility that some mΦ may have resisted depletion and/or the bone marrow rapidly replenished these cells. To assess this possibility, lungs and spleens were also evaluated for the presence of EGFP⁺ cells. As expected, AP20187 treatment markedly depleted EGFP⁺ cells in the lung and to a lesser extent in the spleen (unpublished observation and (Steel et al., 2008). This may reflect the ability of the spleen to function as a haematopoietic organ because treated

mice developed splenomegaly and accumulated CD11b+Gr-1+ EGFP^{low} cells, a phenotype typically expressed by immature monocytes/macrophages. Furthermore, flow cytometric studies demonstrated that these cells were not mΦ but neutrophils based on histological criteria and phenotype (CD45^{high}CD11b+F4/80-Gr-1+). Gr-1+ cells represented infiltrating neutrophils and not activated microglia because they had high expression of CD45 and were F4/80-, whereas microglia were uniformly F4/80+ and remained Gr-1- during VSV encephalitis (data not shown). These results are consistent with the work of Reiss and colleagues who demonstrated an early VSV-induced infiltrate of neutrophils by immunohistochemistry (Bi et al., 1995; Ireland and Reiss, 2006). In normal MAFIA bone marrow essentially all CD45^{high}CD11b+ cells expressed Gr-1 with approximately one-third EGFP^{low/int}. VSV infection resulted in the selective disappearance of Gr-1+EGFP^{low/int} cells from the bone marrow, whereas prior dimerizer treatment resulted in expansion of Gr-1+EGFP^{low/int} cells. It seems likely that these cells emigrated from the bone marrow to infiltrate the brain (and perhaps peritoneum) and contribute to the granulocytic response seen in this organ. This view is consistent with the accumulation of CD45^{high}EGFP^{low/int}F4/80-Gr-1+ cells in the brains of mice depleted of mΦ. In contrast, CD45^{high}CD11b+ cells in the peritoneum were exclusively mΦ. Two mΦ populations based on EGFP expression were present in the normal peritoneum. Macrophages with high EGFP expression were dramatically reduced by VSV infection and this loss was exacerbated by prior dimerizer treatment. Although the number of EGFP^{low/int} mΦ was also reduced by virus infection, this population expanded in mice depleted of mΦ. Thus, peripheral depletion of mΦ may have failed to suppress the inflammatory response in the brain because neutrophils and not mΦ represented the predominant myeloid cell type in the encephalitic brain. Mature neutrophils do not express the CSF-1 receptor (Hume et al., 2002) and would be expected to be insensitive to AP20187 treatment. As noted previously, DCs have low expression (tenfold lower relative to mΦ) of the transgene. This may have prevented significant loss of these essential APCs resulting in normal clonal expansion of CD8+VSV-N T cells in the CLN and subsequent CNS penetration. This speculation, however, will require further investigation.

In striking contrast to this conditional ablation model, intravenous administration of liposome-encapsulated clodronate into naïve MAFIA mice profoundly suppressed VSV encephalitis. The impaired IFN-γ response may reflect the diminished numbers of T cells that infiltrated the brains of mice depleted of mΦ if T cells represent the cellular source of this cytokine. Clodronate treatment was associated with increased morbidity/mortality that did not correlate with impaired viral clearance in the CNS. The different outcome achieved with clodronate versus dimerizer may reflect the different populations targeted by these treatments. In the MAFIA model, AP20187 dimerizer targets mΦ with high c-fms activity and leaves relatively intact cells with low expression levels of the transgene such as DCs and immature and mature granulocytes. Thus neutrophils are not depleted by dimerizer treatment and are available to infiltrate the VSV infected brain. For the same reason, DCs presumably in the draining cervical lymph nodes remain functional and capable of initiating and sustaining a primary T cell-mediated immune response whose progeny accumulate in the CNS. This is consistent with the observed normal clonal expansion of VSV-N T cells detected in the CLN. With respect to clodronate, mΦ engulf liposomes and undergo apoptosis. For reasons that are not clear, neutrophils are not eliminated by clodronate despite their phagocytic activity (Qian et al., 1994) and are therefore available to infiltrate the VSV infected brain. Their diminished numbers in the brain suggests that they may lack the ability to penetrate the BBB. These different outcomes with clodronate versus AP20187 may reflect the observation that clodronate also depletes marginal (CD8-) DCs in the spleen (Leenen et al., 1998) and these cells may migrate to the brain where they play an essential role in the disruption of the BBB. Most DCs in the encephalitic brain express a CD8- phenotype (Figure 4, panels p-r). This view is consistent with the diminished infiltrate observed in

brains of VSV infected transgenic mice depleted of peripheral DCs (Steel et al., 2009) and the failure of Evans blue to penetrate the brain parenchyma of these animals (data not shown). Similar observations have been reported in a murine influenza model where prevention of DC migration from lymph nodes into the lung increased mortality, inhibited viral clearance and pulmonary T cell responses (McGill et al., 2008). The importance of the BBB in regulating encephalitis and viral clearance is highlighted in studies with lethal silver-haired bat rabies virus. Virulent strains do not disrupt the BBB restricting leukocyte influx into the brain parenchyma. Opening the BBB enhanced encephalitis, viral clearance and survival (Roy and Hooper, 2007; Roy et al., 2007).

The brain contains two strategically located m Φ populations, PVM and MM, which represent the major m Φ populations resident in the brain. Because of their strategic location and the observation that CD8⁺ T cell infiltration is markedly enhanced by cognate antigen recognition (Galea et al., 2007), they are ideally suited to function as APCs and to regulate brain inflammation. Their function(s) in the CNS, however, remains poorly defined. Recently, Polfliet and colleagues reported that ICV infusion of liposome-encapsulated clodronate selectively depleted PVM/MM and left resident microglia intact (Polfliet et al., 2001a). Depletion of PVM/MM by clodronate inhibited influx of leukocytes into the CNS during pneumococcal meningitis despite elevated production of relevant chemokines and adhesion molecules (Polfliet et al., 2001b). Clinical symptoms were exacerbated in treated animals likely reflecting elevated production of inflammatory cytokines. Thus, in this bacterial meningitis model PVM and MM play a protective role and suggest that these cells facilitate leukocyte influx at the BBB. In contrast, PVM and MM have been implicated in early disease progression during EAE (Polfliet et al., 2002). As demonstrated in this report, delivery of clodronate directly into the brain profoundly suppressed leukocyte infiltration of non-specific granulocytes and specific CD8⁺ VSV-N T cells. The latter observation was unexpected because clodronate delivered into the brain does not deplete m Φ or DCs in the draining CLN and therefore should not inhibit activation and clonal expansion of VSV-N T cells. Thus, in the VSV model, depletion of CD8-marginal DCs or PVM/MM results in similar consequences on VSV encephalitis, whereas this response remains intact in mice depleted of peripheral m Φ (MAFIA model). How these different cell populations regulate VSV encephalitis is currently unknown. Preliminary PCR array analyses suggest that peripheral DCs are essential for a normal VSV-induced chemokine mRNA response in the CNS (data not shown). Thus, loss of marginal DCs with clodronate may have contributed to the impaired responses seen in these mice. The observation that depletion of PVMs appears to impair VSV encephalitis in a similar manner suggests that these two populations regulate VSV encephalitis in an apparent non-redundant fashion.

Studies with clodronate suggest that a robust leukocyte infiltrate is not essential for VSV clearance and survival. This implies that efficient CNS viral clearance mechanisms exist independent of infiltrating blood-derived leukocytes. This notion is supported by the observation that astrocytes display the appropriate TLRs (TLR4/7) for VSV recognition and triggering of these receptors leads to production of the antiviral protein IFN α (Carpentier et al., 2005; McKimmie and Fazakerley, 2005). Microglia possess similar properties and functions (Olson and Miller, 2004). Recent studies in mice with a cell type-specific IFN receptor deletion in neuroectodermal cells of the CNS demonstrate the importance of local production of type I IFN for VSV clearance and survival. Thus these mice die within 2–3 days post infection, whereas normal mice survive this dose of infection (Detje et al., 2009). Interestingly, IFN α protein levels in the brain of these mice were too low to detect by ELISA, an observation that is consistent with prior reports that IFN α protein was detected in the blood but not in the CNS during VSV encephalitis (Ciavarrá et al., 2005; Trottier et al., 2007). Resident astrocytes can also produce IFN- γ (Lau and Yu, 2001) which inhibits VSV replication in the CNS (Kundig et al., 1993) likely by IFN- γ -dependent upregulation of type

iNOS (Komatsu et al., 1996; Komatsu et al., 1999). Viral clearance and host recovery is associated with NOS-1 expression in neurons and not other isoforms despite abundant and early expression of inducible nitric oxide synthase (iNOS, NOS-2) in the OB (Komatsu et al., 1999). In view of the exquisite sensitivity of VSV to the antiviral activity of types I/II IFNs, it seems likely that this system contributes significantly to survival in the absence of a significant infiltrate of leukocytes. In addition to the innate response, adaptive immunity clearly contributes to VSV clearance and long-term survival. Thus, nude mice are healthy initially following intranasal VSV infection because their innate defences are still intact, but ultimately succumb between days 10–14 post infection to doses of VSV that are not lethal to immunocompetent mice. CD4⁺ and CD8⁺ T cells infiltrate the brain around days 4–5 corresponding to the appearance of IFN- γ mRNA in the brain (Ireland and Reiss, 2006). Mechanistically, VSV replication and viral protein synthesis in neurons are inhibited by IFN- γ both *in vitro* and *in vivo* which correlates with upregulation of NOS-1 protein levels and increased production of NO (Komatsu et al., 1996; Komatsu et al., 1999).

In summary, we have utilized two different approaches to deplete m Φ *in vivo* to access their role in VSV encephalitis. When peripheral m Φ were depleted in a conditional ablation transgenic model (MAFIA), VSV encephalitis was not impaired relative to control mice. In striking contrast, treatment with clodronate-encapsulated liposomes, which also depletes CD8⁻ marginal DCs, inhibited VSV encephalitis. Similar results were observed when mice were given clodronate via the ICV route where only PVM and MM were depleted. In all 3 experimental conditions, viral clearance remained relatively normal but not predictive of morbidity/mortality. Thus, VSV encephalitis is regulated in an apparent non-redundant fashion by two distinct phagocytic populations, CD8⁻ DCs and PVMs, that reside in the marginal sinus of the spleen and perivascular spaces in the brain, respectively. Gene expression studies are currently underway to determine why peripheral DCs are essential for an inflammatory response in the CNS. Quantitative PCR findings indicate that VSV encephalitis is associated with a DC-dependent induction of chemokines and proinflammatory cytokines (unpublished observation). Thus, DCs regulate leukocyte infiltration because they are essential for chemokine production in the CNS, whereas PVMs provide an unknown non-redundant function. Based on these and other studies, we propose a model where resident glial cells produce chemokines but only after receiving a signal(s) from infiltrating DCs, whereas PVMs are required for proinflammatory cytokine production and disruption of the BBB facilitating leukocyte entry into the brain parenchyma. At the dose used in this study, innate antiviral mechanisms are sufficient for viral clearance. We further suggest that morbidity/mortality occurs despite viral clearance because brain PVMs produce proinflammatory cytokines (TNF α , IL-1). Thus, clodronate given via the intravenous route leaves brain PVMs intact resulting in morbidity, whereas ICV clodronate eliminates these cells and mice remain healthy. Studies are currently underway to test the validity of this model.

Acknowledgments

The authors would like to recognize the expert technical assistance of Suzanne M. Hahto. We are also grateful to Ariad Pharmaceuticals, Inc. for supplying the AP20187 dimerizer. This work was supported by a grant from the NIH (RO1AI048700) to R.P.C.

References

- Barna M, Komatsu T, Bi Z, Reiss CS. Sex differences in susceptibility to viral infection of the central nervous system. *J Neuroimmunol.* 1996; 67:31–39. [PubMed: 8707928]
- Battegay M, Bachmann MF, Burkhart C, Viville S, Benoist C, Mathis D, Hengartner H, Zinkernagel RM. Antiviral immune responses of mice lacking MHC class II or its associated invariant chain. *Cell Immunol.* 1996; 167:115–121. [PubMed: 8548834]

- Bi Z, Barna M, Komatsu T, Reiss CS. Vesicular stomatitis virus infection of the central nervous system activates both innate and acquired immunity. *J Virol.* 1995; 69:6466–6472. [PubMed: 7545248]
- Burnett SH, Kershner EJ, Zhang J, Zeng L, Straley SC, Kaplan AM, Cohen DA. Conditional macrophage ablation in transgenic mice expressing a Fas-based suicide gene. *J Leukoc Biol.* 2004; 75:612–623. [PubMed: 14726498]
- Carpentier PA, Begolka WS, Olson JK, Elhofy A, Karpus WJ, Miller SD. Differential activation of astrocytes by innate and adaptive immune stimuli. *Glia.* 2005; 49:360–374. [PubMed: 15538753]
- Charan S, Huegin AW, Cerny A, Hengartner H, Zinkernagel RM. Effects of cyclosporin A on humoral immune response and resistance against vesicular stomatitis virus in mice. *J Virol.* 1986; 57:1139–1144. [PubMed: 3005615]
- Ciavarra RP, Stephens A, Nagy S, Sekellick M, Steel C. Evaluation of immunological paradigms in a virus model: are dendritic cells critical for antiviral immunity and viral clearance? *J Immunol.* 2006; 177:492–500. [PubMed: 16785546]
- Ciavarra RP, Taylor L, Greene AR, Yousefieh N, Horeth D, van Rooijen N, Steel C, Gregory B, Birkenbach M, Sekellick M. Impact of macrophage and dendritic cell subset elimination on antiviral immunity, viral clearance and production of type 1 interferon. *Virology.* 2005
- Ciavarra RP, Tedeschi B. Priming antiviral cytotoxic T lymphocytes: requirement for CD4+ cells is dependent on the antigen presenting cell in vivo. *Cell Immunol.* 1994; 157:132–143. [PubMed: 7913664]
- Coons WJ, Vorhies RW, Johnson TC. An immune cell population that responds to beta-endorphin and is responsible for protecting nude mice from the fatal consequences of a virus infection of the central nervous system. *J Neuroimmunol.* 1991; 34:133–141. [PubMed: 1655824]
- Detje CN, Meyer T, Schmidt H, Kreuz D, Rose JK, Bechmann I, Prinz M, Kalinke U. Local type I IFN receptor signaling protects against virus spread within the central nervous system. *J Immunol.* 2009; 182:2297–2304. [PubMed: 19201884]
- Forger JM 3rd, Bronson RT, Huang AS, Reiss CS. Murine infection by vesicular stomatitis virus: initial characterization of the H-2d system. *J Virol.* 1991; 65:4950–4958. [PubMed: 1651414]
- Frei K, Malipiero UV, Leist TP, Zinkernagel RM, Schwab ME, Fontana A. On the cellular source and function of interleukin 6 produced in the central nervous system in viral diseases. *Eur J Immunol.* 1989; 19:689–694. [PubMed: 2543584]
- Galea I, Bernardes-Silva M, Forse PA, van Rooijen N, Liblau RS, Perry VH. An antigen-specific pathway for CD8 T cells across the blood-brain barrier. *J Exp Med.* 2007; 204:2023–2030. [PubMed: 17682068]
- Galea I, Palin K, Newman TA, Van Rooijen N, Perry VH, Boche D. Mannose receptor expression specifically reveals perivascular macrophages in normal, injured, and diseased mouse brain. *Glia.* 2005; 49:375–384. [PubMed: 15538754]
- Hume DA, Ross IL, Himes SR, Sasmono RT, Wells CA, Ravasi T. The mononuclear phagocyte system revisited. *J Leukoc Biol.* 2002; 72:621–627. [PubMed: 12377929]
- Hummer HJ, Coons WJ, Watts SA, Johnson TC. Beta-endorphin alters the course of central nervous system disease induced by a temperature-sensitive vesicular stomatitis virus in reconstituted nude mice. *J Neuroimmunol.* 1990; 28:73–82. [PubMed: 2160476]
- Huneycutt BS, Bi Z, Aoki CJ, Reiss CS. Central neuropathogenesis of vesicular stomatitis virus infection of immunodeficient mice. *J Virol.* 1993; 67:6698–6706. [PubMed: 8105106]
- Ireland DD, Reiss CS. Gene expression contributing to recruitment of circulating cells in response to vesicular stomatitis virus infection of the CNS. *Viral Immunol.* 2006; 19:536–545. [PubMed: 16987071]
- Komatsu T, Bi Z, Reiss CS. Interferon-gamma induced type I nitric oxide synthase activity inhibits viral replication in neurons. *J Neuroimmunol.* 1996; 68:101–108. [PubMed: 8784266]
- Komatsu T, Ireland DD, Chen N, Reiss CS. Neuronal expression of NOS-1 is required for host recovery from viral encephalitis. *Virology.* 1999; 258:389–395. [PubMed: 10366576]
- Kundig TM, Hengartner H, Zinkernagel RM. T cell-dependent IFN-gamma exerts an antiviral effect in the central nervous system but not in peripheral solid organs. *J Immunol.* 1993; 150:2316–2321. [PubMed: 8450214]

- Lau LT, Yu AC. Astrocytes produce and release interleukin-1, interleukin-6, tumor necrosis factor alpha and interferon-gamma following traumatic and metabolic injury. *J Neurotrauma*. 2001; 18:351–359. [PubMed: 11284554]
- Leenen PJ, Radosevic K, Voerman JS, Salomon B, van Rooijen N, Klatzmann D, van Ewijk W. Heterogeneity of mouse spleen dendritic cells: in vivo phagocytic activity, expression of macrophage markers, and subpopulation turnover. *J Immunol*. 1998; 160:2166–2173. [PubMed: 9498754]
- Marvaldi JL, Lucas-Lenard J, Sekellick MJ, Marcus PI. Cell killing by viruses. IV. Cell killing and protein synthesis inhibition by vesicular stomatitis virus require the same gene functions. *Virology*. 1977; 79:267–280. [PubMed: 194405]
- McGill J, Van Rooijen N, Legge KL. Protective influenza-specific CD8 T cell responses require interactions with dendritic cells in the lungs. *J Exp Med*. 2008; 205:1635–1646. [PubMed: 18591411]
- McKimmie CS, Fazakerley JK. In response to pathogens, glial cells dynamically and differentially regulate Toll-like receptor gene expression. *J Neuroimmunol*. 2005; 169:116–125. [PubMed: 16146656]
- Nansen A, Marker O, Bartholdy C, Thomsen AR. CCR2+ and CCR5+ CD8+ T cells increase during viral infection and migrate to sites of infection. *Eur J Immunol*. 2000; 30:1797–1806. [PubMed: 10940868]
- Olson JK, Miller SD. Microglia initiate central nervous system innate and adaptive immune responses through multiple TLRs. *J Immunol*. 2004; 173:3916–3924. [PubMed: 15356140]
- Polfliet MM, Goede PH, van Kesteren-Hendriks EM, van Rooijen N, Dijkstra CD, van den Berg TK. A method for the selective depletion of perivascular and meningeal macrophages in the central nervous system. *J Neuroimmunol*. 2001a; 116:188–195. [PubMed: 11438173]
- Polfliet MM, van de Veerdonk F, Dopp EA, van Kesteren-Hendriks EM, van Rooijen N, Dijkstra CD, van den Berg TK. The role of perivascular and meningeal macrophages in experimental allergic encephalomyelitis. *J Neuroimmunol*. 2002; 122:1–8. [PubMed: 11777538]
- Polfliet MM, Zwijnenburg PJ, van Furth AM, van der Poll T, Dopp EA, Renardel de Lavalette C, van Kesteren-Hendriks EM, van Rooijen N, Dijkstra CD, van den Berg TK. Meningeal and perivascular macrophages of the central nervous system play a protective role during bacterial meningitis. *J Immunol*. 2001b; 167:4644–4650. [PubMed: 11591794]
- Pozzi LA, Maciaszek JW, Rock KL. Both dendritic cells and macrophages can stimulate naive CD8 T cells in vivo to proliferate, develop effector function, and differentiate into memory cells. *J Immunol*. 2005; 175:2071–2081. [PubMed: 16081773]
- Qian Q, Jutila MA, Van Rooijen N, Cutler JE. Elimination of mouse splenic macrophages correlates with increased susceptibility to experimental disseminated candidiasis. *J Immunol*. 1994; 152:5000–5008. [PubMed: 8176217]
- Reiss CS, Plakhov IV, Komatsu T. Viral replication in olfactory receptor neurons and entry into the olfactory bulb and brain. *Ann N Y Acad Sci*. 1998; 855:751–761. [PubMed: 9929681]
- Rieser C, Ramoner R, Bock G, Deo YM, Holtl L, Bartsch G, Thurnher M. Human monocyte-derived dendritic cells produce macrophage colony-stimulating factor: enhancement of c-fms expression by interleukin-10. *Eur J Immunol*. 1998; 28:2283–2288. [PubMed: 9710206]
- Roy A, Hooper DC. Lethal silver-haired bat rabies virus infection can be prevented by opening the blood-brain barrier. *J Virol*. 2007; 81:7993–7998. [PubMed: 17507463]
- Roy A, Phares TW, Koprowski H, Hooper DC. Failure to open the blood-brain barrier and deliver immune effectors to central nervous system tissues leads to the lethal outcome of silver-haired bat rabies virus infection. *J Virol*. 2007; 81:1110–1118. [PubMed: 17108029]
- Russell RG, Rogers MJ. Bisphosphonates: from the laboratory to the clinic and back again. *Bone*. 1999; 25:97–106. [PubMed: 10423031]
- Sekellick MJ, Marcus PI. Persistent infection. II. Interferon-inducing temperature-sensitive mutants as mediators of cell sparing: possible role in persistent infection by vesicular stomatitis virus. *Virology*. 1979; 95:36–47. [PubMed: 220798]

- Steel CD, Hahto SM, Ciavarra RP. Peripheral dendritic cells are essential for both the innate and adaptive antiviral immune responses in the central nervous system. *Virology*. 2009; 387:117–126. [PubMed: 19264338]
- Steel CD, Stephens AL, Hahto SM, Singletary SJ, Ciavarra RP. Comparison of the lateral tail vein and the retro-orbital venous sinus as routes of intravenous drug delivery in a transgenic mouse model. *Lab Anim (NY)*. 2008; 37:26–32. [PubMed: 18094699]
- Trottier MD, Lyles DS, Reiss CS. Peripheral, but not central nervous system, type I interferon expression in mice in response to intranasal vesicular stomatitis virus infection. *J Neurovirol*. 2007; 13:433–445. [PubMed: 17994428]
- Turner DL, Cauley LS, Khanna KM, Lefrancois L. Persistent antigen presentation after acute vesicular stomatitis virus infection. *J Virol*. 2007; 81:2039–2046. [PubMed: 17151119]
- Van Rooijen N, Kors N, vd Ende M, Dijkstra CD. Depletion and repopulation of macrophages in spleen and liver of rat after intravenous treatment with liposome-encapsulated dichloromethylene diphosphonate. *Cell Tissue Res*. 1990; 260:215–222. [PubMed: 2141546]
- van Rooijen N, Sanders A, van den Berg TK. Apoptosis of macrophages induced by liposome-mediated intracellular delivery of clodronate and propamidine. *J Immunol Methods*. 1996; 193:93–99. [PubMed: 8690935]

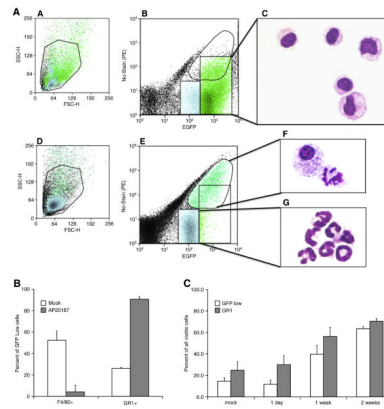


Figure 1. Dimerizer treatment depletes EGFP^{high} cells in MAFIA mice and induces a potent and sustained accumulation of granulocytes in the peritoneal cavity

MAFIA mice were either untreated (mock) or depleted of m Φ by AP20187 treatment and the following day peritoneal exudates cells (PECs) harvested for flow cytometric analysis. (panel A) The top and bottom 3 panels represent PECs isolated from untreated and AP20187 treated mice, respectively. Panels a and d show the forward and side scatter plots with the region indicating viable cells. Cells from the GFP^{high} region in panels b and e (box and circle, respectively) were sorted, subjected to cytopsin centrifugation and stained with May-Grunwald/Geimsa for microscopy (panels c and f). The GFP^{low} population in dimerizer treated mice was also sorted and evaluated by microscopy (panel g). In panel B, viable EGFP^{low} cells were gated and expression of F4/80 and Gr-1 evaluated by flow cytometry. The decrease in F4/80 and increase in Gr-1 expression was statistically significant (T test, $\alpha=0.001$). (panel C) Sustained accumulation of EGFP^{low} and Gr-1+ in the peritoneum of MAFIA mice treated with AP20187. Day 1 values were not statistically significant for EGFP^{low} and Gr-1+ cells (T test, $\alpha=0.1$). However, statistically significant differences existed between the EGFP^{low} and Gr-1+ cells at 1 and 2 weeks in AP20187 versus mock treated mice ($\alpha=0.05$)

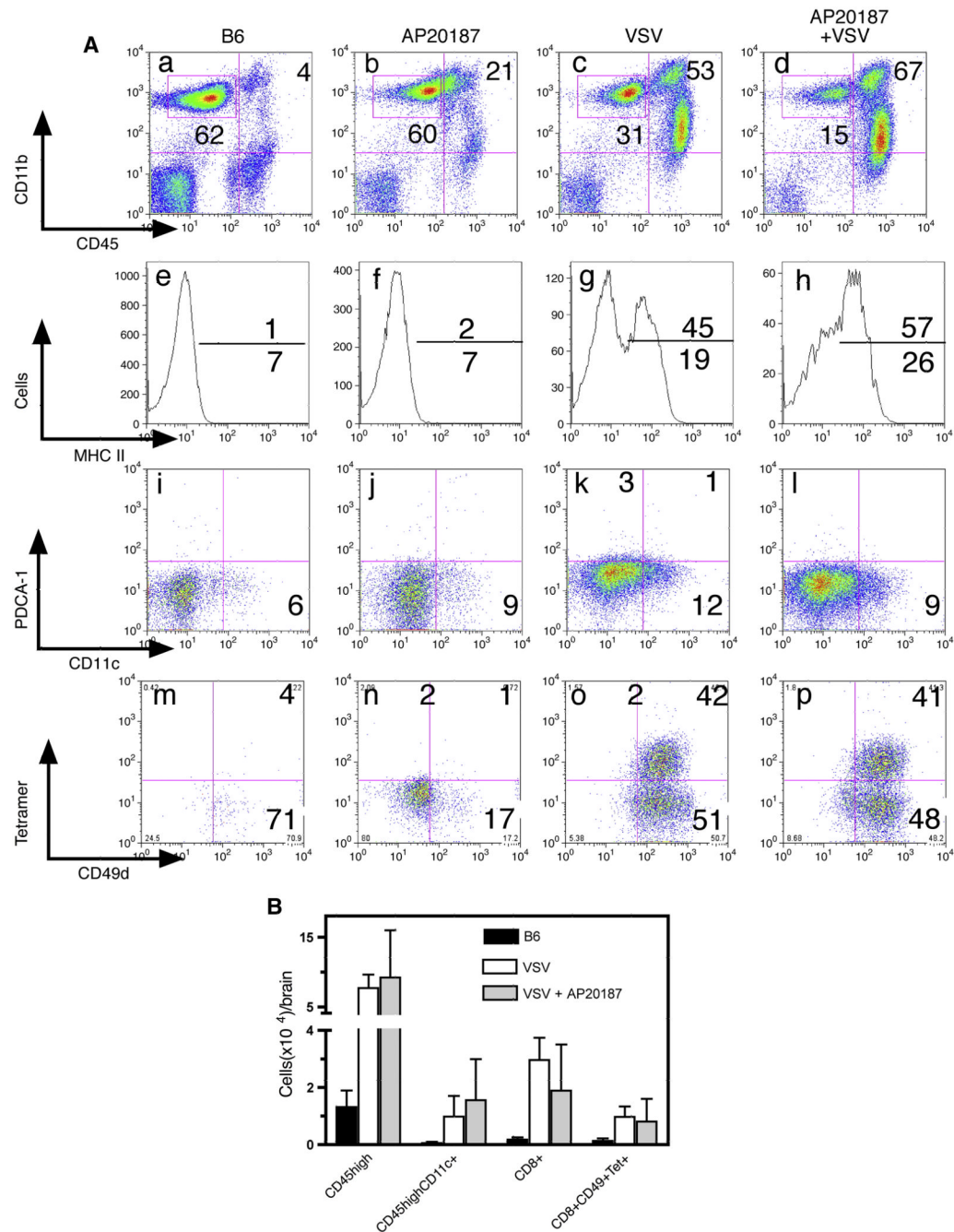


Figure 2. VSV encephalitis progresses normally following acute depletion of peripheral macrophages

(panel A) MAFIA mice (5 mice/group) were treated for 5 days s with dimerizer and the following day given a single intranasal application of VSV. Naïve B6 mice were used to define EGFP-cells and to assess the number of leukocytes present in uninfected brains (first column). MAFIA mice were given just AP20187 (2nd column), VSV only (3rd column) or AP20187 + VSV (4th column). Eight days post-infection, leukocytes were isolated from brains, viable cells gated based on forward and side scatter characteristics and phenotyped by multiparameter flow cytometry. Microglia were gated as CD45^{low/int}CD11b⁺ (box, panels a–d). The activation status of microglia was then accessed by MHC class II antigen

expression (panels e–h). Conventional and pDCs were identified in a CD45^{high}CD11b⁺ gate using the indicated mAbs (panels i–l). VSV-N T cells were identified in gated CD8⁺ cells by class I tetramer binding and co-expression of CD49d (panels m–p). (panel B) Data from this and two additional experiments was pooled to calculate specific cell recoveries from the brain (expressed as mean \pm SEM) following the indicated treatments. No significant differences in cell recoveries were detected between VSV infected mice that were either untreated or treated with AP20187.

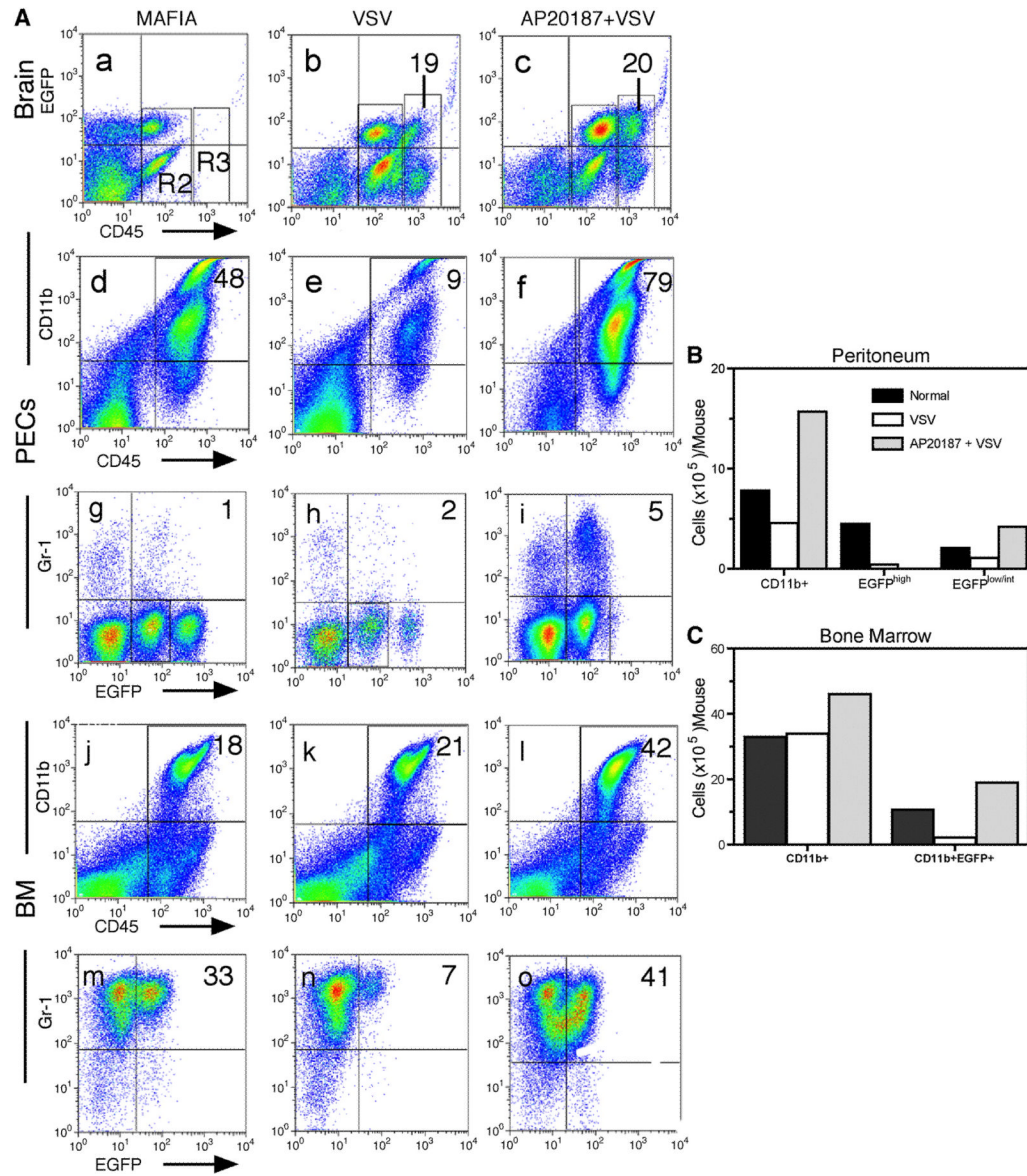


Figure 3. Sustained depletion of EGFP+ macrophages in MAFIA mice during VSV encephalitis
 MAFIA mice (4–6 mice/group) were treated with AP20187 intravenously for 5 consecutive days and on the following day given an intranasal application of VSV (2×10^5 PFU). Six days post infection, brain leukocytes were isolated along with bone marrow and peritoneal exudates cells. Cells were incubated with the indicated mAbs and then phenotyped by flow cytometry. (A) Cells were stained with mAbs to CD45 and CD11b to characterize the inflammatory infiltrate in the brain (panels a–c) and to evaluate the consequences of dimerizer treatment on leukocytes derived from the peritoneum (panels d–f) and bone marrow (panels j–l). Co-expression of Gr-1 and EGFP on gated CD45^{high}CD11b+ cells was then evaluated on cells derived from the peritoneum (panels g–i) and bone marrow (m–o). (B) The absolute number of cells of the indicated phenotype was calculated by multiplying total leukocyte recoveries x percentage of cells with the selected phenotype. The experiment was repeated a second time and yielded comparable results.

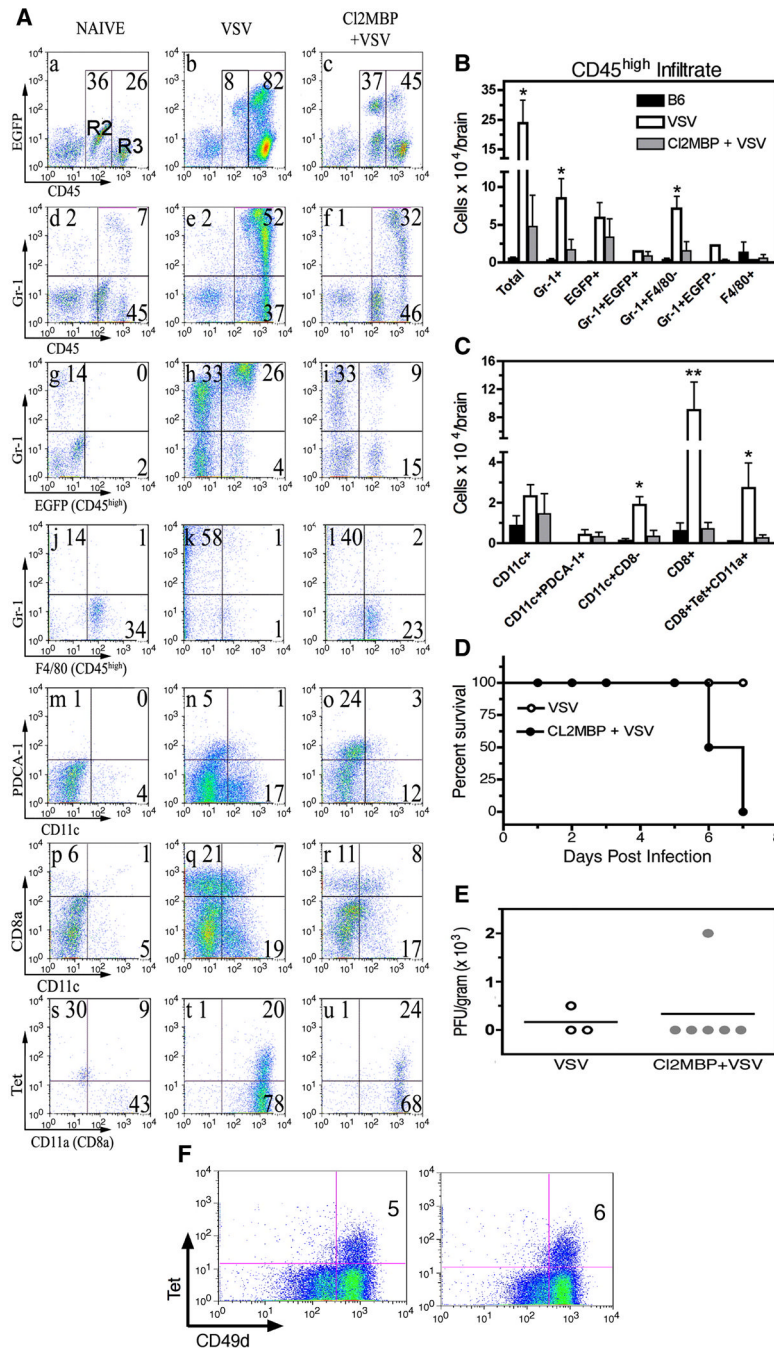


Figure 4. Clodronate markedly suppresses viral encephalitis but not viral clearance in the CNS
 Six MAFIA mice received a single injection (retro-orbital sinus) of liposome-encapsulated clodronate and the following day inoculated with VSV (5×10^5 PFU) via the intranasal route. Controls were either uninfected B6 (3 mice) or MAFIA mice given just VSV (4 mice). Seven days post infection peripheral organs were pooled, homogenized and single cell suspensions prepared from spleen and CLNs. Brain leukocytes were enriched on Percoll gradients. Cells were stained with the indicated mAbs and analyzed by multi-parameter flow cytometry. (panel A) Viable leukocytes were first defined based on forward and side scatter characteristics (Region 1, R1) and within this gate microglia and the cellular infiltrate defined as CD45^{low/int} and CD45^{high} cells, respectively (R2 and R3, panels a–c). The

granulocyte composition of the brain was assessed broadly using the R1 gate (panels d–f) and then specificity in the infiltrate (R3, panels g–l). Conventional, pDCs (panels m–o) and CD11c+CD8+/- DCs (panels p–r) were also identified in the R1 gate. To identify VSV-N T cells, tetramer binding and expression of the activation marker CD11a were determined on gated CD8+ cells (panels s–u). (panels B, C). Cell recoveries from encephalitic brains of untreated mice and mice treated with clodronate. Error bars represent SEM of a minimum of 3 experiments with 4–10 mice per group. Recoveries were calculated using either R3 (B) or R1 gates (C). ** $p < 0.01$ versus Cl2MBP + VSV, * $p < 0.05$ versus Cl2MBP + VSV calculated by *t* test (GraphPad Prism 4). (panel D) Enhanced morbidity/mortality associated with VSV encephalitis in mice treated with liposome-encapsulated clodronate. (panel E) Depletion of peripheral m Φ did not inhibit viral clearance from the CNS. Comparable viral titers were obtained when this experiment was repeated using 4–6 mice/group. (panel F) Clonal expansion of VSV-N T cells in the draining CLN is not impaired in mice depleted of peripheral m Φ (panel F). Tetramer+ (Tet+) cells were identified in gated CD8+ cells.

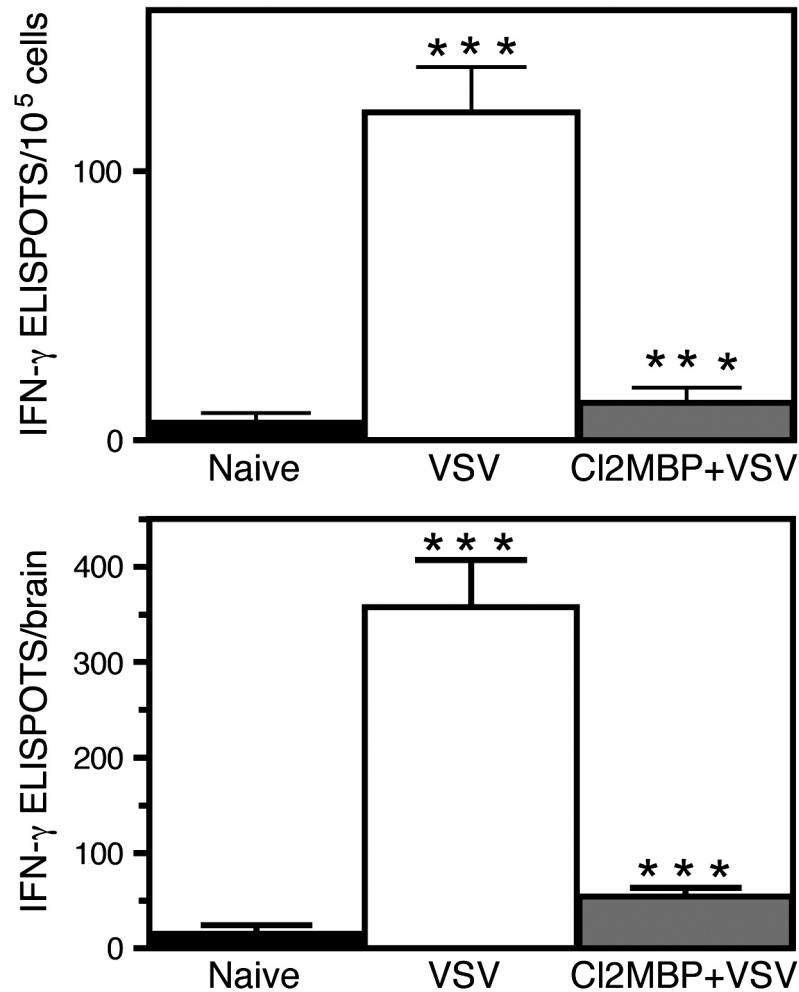


Figure 5. Ablation of peripheral macrophages suppresses the VSV-induced interferon gamma response in the CNS

MAFIA mice (3–6 per group) were either untreated or given intravenous clodronate. The following day mice were infected with VSV via the intranasal route and brain leukocytes isolated seven days post infection. An IFN- γ ELISPOT assay was then performed as previously described using six replicates per input cell number (Ciavarrà et al., 2006). Cells were not re-stimulated with VSV *in vitro* to more accurately estimate the number of cytokine-producing cells *in vivo*. Data are expressed as either the number of cytokine-producing cells/10⁵ cells (upper panel) or total number of cytokine-producing cells per brain (bottom panel).

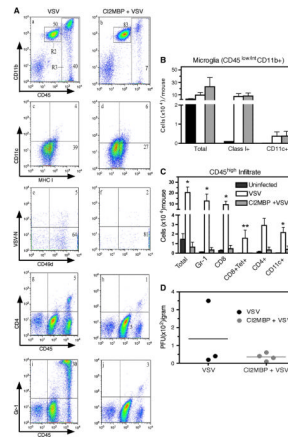


Figure 6. Impaired antiviral immune responses in the CNS of mice rendered deficient of perivascular macrophages

MAFIA mice were depleted of perivascular m Φ by surgical administration of 8 μ L clodronate-liposomes into the left lateral ventricle of the brain (ICV injection). Mice were allowed to recover from surgery for 3 days and then given an intranasal application of VSV. Seven days post-infection, mice were euthanized to harvest brain tissue for plaque assay or flow cytometry. (panel A) Multicolour flow cytometry was performed on brains leukocytes derived from VSV infected mice that were either untreated (VSV, panels a, c, e, g, i) or given a prior ICV injection of clodronate (Cl2MBP + VSV, panels b, d, f, h, j). Microglia were gated as CD45^{int/low} (R2, panels a, b) and co-expression of CD11c and MHC class I determined (panels c, d). T cells specific for VSV were defined as tetramer+CD49d+ cells located in gated CD8+ cells (panels e, f). Infiltrating CD4+ cells with unknown specificity were also detected in brains of infected mice (panels g, h). (panel B) Cell recoveries of microglia expressing the indicated phenotype. Error bars represent SEM of experiments with 4–6 mice per group. (panel C) Calculated cell recoveries of the indicated leukocyte populations. **p < 0.01 versus Cl2MBP + VSV, *p < 0.05 versus Cl2MBP + VSV calculated by *t* test (GraphPad Prism 4). (panel D) VSV titers in the brains of untreated (VSV) or clodronate treated mice (Cl2MBP+VSV). Similar viral titers were obtained when this experiment was repeated using 4–6 mice/group.

TABLE I

Cell Populations Targeted by the Indicated Treatments

Treatment	Liver	Lung	Spleen	BM	PC	LN	Brain	Blood
CL2MBP IV	Kupffer	ND	m ϕ \pm DC	m ϕ	m ϕ	ND	ND	mono
CL2MBP ICV	ND	ND	ND	ND	ND	ND	ND	PVM/MM
AP20187	Kupffer	m ϕ	m ϕ \pm DC	m ϕ	m ϕ	?	ND	mono

PC (peritoneal cavity); ND (none detected); mono (monocytes); PVM/MM (perivascular macrophage/meningeal macrophage)